J|A|C|S
ARTICLES
Published on Web 02/21/2008

Processing Additives for Improved Efficiency from Bulk Heterojunction Solar Cells

Jae Kwan Lee,[†] Wan Li Ma,[†] Christoph J. Brabec,[‡] Jonathan Yuen,[†] Ji Sun Moon,[†] Jin Young Kim,[†] Kwanghee Lee,[†] Guillermo C. Bazan,[†] and Alan J. Heeger*,[†]

Center for Polymers and Organic Solids, University of California at Santa Barbara, Santa Barbara, California 93106, and Konarka Technologies Austria, Altenbergerstrasse 69, A-4-4- Linz, Austria

Received November 13, 2007; E-mail: ajhe@physics.ucsb.edu

Abstract: Two criteria for processing additives introduced to control the morphology of bulk heterojunction (BHJ) materials for use in solar cells have been identified: (i) selective (differential) solubility of the fullerene component and (ii) higher boiling point than the host solvent. Using these criteria, we have investigated the class of 1,8-di(R)octanes with various functional groups (R) as processing additives for BHJ solar cells. Control of the BHJ morphology by selective solubility of the fullerene component is demonstrated using these high boiling point processing additives. The best results are obtained with R = Iodine (I). Using 1,8-diiodooctane as the processing additive, the efficiency of the BHJ solar cells was improved from 3.4% (for the reference device) to 5.1%.

Introduction

Polymer solar cells based on bulk heterojunction (BHJ) materials comprising π-conjugated (semiconducting) polymers and fullerene derivatives have demonstrated promising performance.[1−9] In order to understand the BHJ materials and to optimize the efficiency of BHJ photovoltaic cells, the nanostructure has been studied using transmission electron microscopy (TEM), X-ray diffraction (XRD), nuclear magnetic resonance (NMR), and atomic force microscopy (AFM); the achievement of high efficiency BHJ polymer solar cells requires the existence of interpenetrating channel-like domains which separate the polymer and fullerene phases.[7−10,12−16]

After annealing at elevated temperatures, relatively high efficiency solar cells have been demonstrated using regioregular poly(3-hexylthiophene) (rrP3HT) with [6,6]-phenyl-C61-butyric acid methyl ester (C_{61}-PCBM) and poly[2-methoxy-5-(3,7-dimethyloctyloxy)]-1,4-phenylene-vinylene (MDMO-PPV) with C_{61}-PCBM; the annealed BHJ films fabricated with these materials show well-defined bicontinuous interpenetrating networks. The importance of the solvent in determining the BHJ morphology has also been established, with finer phase separation in films cast from chlorobenzene than in films cast from toluene.[10,11]

The addition of alkanedithiols into the solvent was recently shown to improve the performance of BHJ solar cells.[18] By incorporating a few volume percent of alkanedithiol into the chlorobenzene from which BHJ films comprising the low band gap polymer [2,6-(4,4-bis(2-ethylhexyl)-4*H*-cyclopenta[2,1-b;3,4-b′]-dithiophene)-*alt*-4,7-(2,1,3-benzothiadiazole)] (PCPDTBT) and C_{71}-PCBM are cast, the power conversion efficiency (AM 1.5G conditions) was increased from 2.8% to 5.5%.[17,18] Although evidence of the formation of phase separated BHJ materials was clearly observed, there was no alkanedithiol in thoroughly dried films. Thus, although the alkanedithiols functioned as "processing additives" for improving the morphology of the BHJ material, the mechanism by which this occurred was unknown.

Herein, we clarify the mechanism by which processing additives control the morphology, and using the insight provided

[†] University of California at Santa Barbara.
[‡] Konarka Technologies Austria.

(1) Sacriciftci, N. S.; Smilowitz, L.; Heeger, A. J.; Wudl, F. *Science* **1992**, *258*, 1474−1476.
(2) Yu, G.; Gao, J.; Hummelen, J. C.; Wudl, F.; Heeger, A. J. *Science* **1995**, *270*, 1789−1791.
(3) Shaheen, S. E.; Brabec, C. J.; Sariciftci, N. S.; Padinger, F.; Fromherz, T.; Hummelen, J. C. *Appl. Phys. Lett.* **2001**, *78*, 841−843.
(4) Padinger, F.; Rittberger, R. S.; Sariciftci, N. S. *Adv. Funct. Mater.* **2003**, *13*, 85−88.
(5) Al-lbrahim, M.; Ambacher, O.; Sensfuss, S.; Gobsch, G. *Appl. Phys. Lett.* **2005**, *86*, 201120−3.
(6) Kim, Y.; Choulis, S. A.; Nelson, J.; Bradley, D. D. C.; Cook, S.; Durrant, J. R. *Appl. Phys. Lett.* **2005**, *86*, 063502−3.
(7) Hoppe, H.; Saricitfci, N. S. *J. Mater. Chem.* **2006**, *16*, 45−61.
(8) Savenije, T. J.; Kroeze, J. E.; Yang, X.; Loos, J. *Adv. Funct. Mater.* **2005**, *15*, 1260−1266.
(9) Yang, C.; Hu, J. G.; Heeger, A. J. *J. Am. Soc. Chem.* **2006**, *128*, 12007−12013.
(10) Ma, W.; Yang, C.; Gong, X.; Lee, K.; Heeger, A. J. *Adv. Funct. Mater.* **2005**, *15*, 1617−1622.
(11) Hoppe, M.; Niggemann, M.; Winder, C.; Kraut, J.; Hiesgen, R.; Hinch, A.; Meissner, D.; Sariciftci, N. S. *Adv. Funct. Mater.* **2004**, *14*, 1005−1011.
(12) Kline, R. J.; Mcgehee, M. D.; Toney, M. F. *Nat. Mater.* **2006**, *5*, 222−228.
(13) Sivula, K.; Ball, Z. T.; Watanabe, N.; Frechet, J. M. J. *Adv. Mater.* **2006**, *18*, 206−210.
(14) Reyes-Reyes, M.; Kim, K.; Dewald, J.; Lopez-Sandoval, R.; Avadhanula, A.; Curran, S.; Carroll, D. *Org. Lett.* **2005**, *7*, 5749−5752.
(15) Zhokhavets, U.; Erb, T.; Hoppe, H.; Gobsch, G.; Sariciftci, N. S. *Thin Solid Film* **2006**, *496*, 679−682.
(16) Camaioni, N.; Ridolfi, G.; Casalbore-Miceli, G.; Possamai, G.; Maggini, M. *Adv. Mater.* **2002**, *14*, 1735−1738.
(17) Peet, J.; Soci, C.; Coffin, R. C.; Nguyen, T. Q.; Mikhailovsky, A.; Moses, D.; Bazan, G. C. *Appl. Phys. Lett.* **2006**, *89*, 252105−252107.
(18) Peet, J.; Kim, J. Y.; Coates, N. E.; Ma, W. L.; Moses, D.; Heeger, A. J.; Bazan, G. C. *Nat. Mater.* **2007**, *6*, 497−500.

Scheme 1 [a]

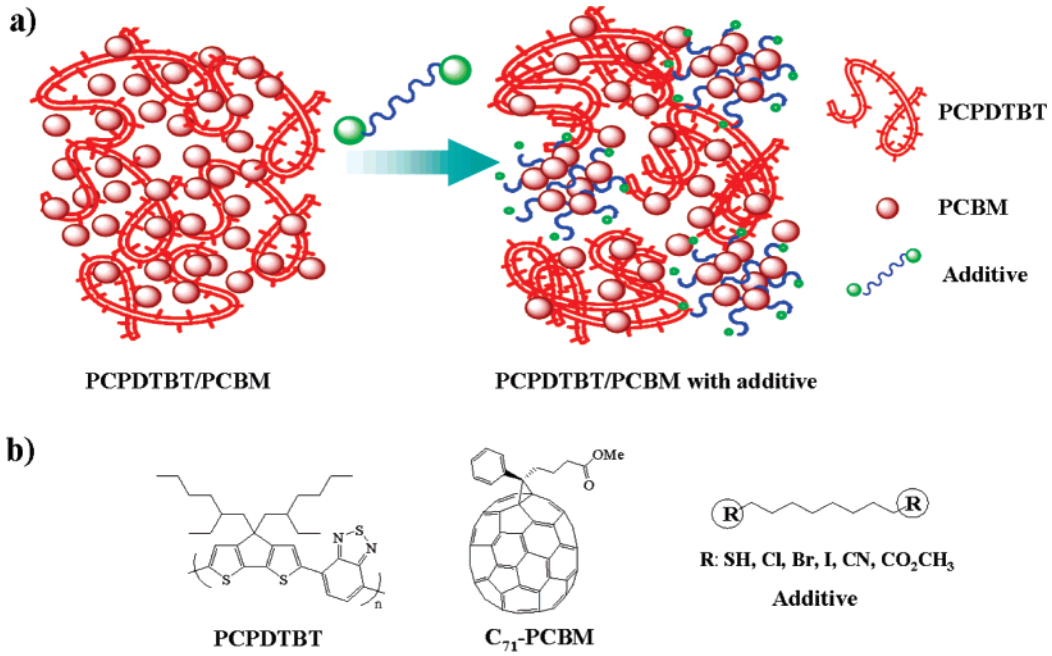

[a] Schematic depiction of the role of the processing additive in the self-assembly of bulk heterojunction blend materials (a) and structures of PCPDTBT, C_{71}-PCBM, and additives (b).

by the mechanism, we identify an entire class of processing additives which yields still higher efficiency solar cells than those fabricated with 1,8-octanedithiol as the processing additive.

The alkanedithiols do not react with either the polymer or the fullerene; they function as processing additives. As indicated by Fourier transform infrared (FTIR) spectroscopy, Raman spectroscopy, and X-ray photoelectron spectroscopy (XPS), the alkanedithiol is removed while drying the film under high vacuum.[18] We find that the alkanedithiol selectively dissolves the PCBM; C_{61}-PCBM and C_{71}-PCBM are readily dissolved in alkanedithiol, but P3HT and PCPDTBT are not soluble in alkanedithiol. Because the fullerenes are selectively dissolved in alkanedithiol, three separate phases are formed during the process of liquid−liquid phase separation and drying: a fullerene−alkanedithiol phase, a polymer aggregate phase, and a polymer−fullerene phase. In addition, because the alkanedithiol has a higher boiling point than the chlorobenzene host solvent, the PCBM tends to remain in solution (during drying) longer than the semiconducting polymer, thereby enabling control of the phase separation and the resulting morphology of the BHJ material; see Scheme 1.

Figure 1 shows the UV−visible absorption spectrum of PCPDTBT/C_{71}-PCBM BHJ films spin-cast from a blend solution containing 2.5% 1,8-octanedithiol in chlorobenzene (black) and the UV−vis spectrum of a PCPDTBT network film which has been soaked in alkanedithiol to remove the C_{71}-PCBM (red). The absorption spectrum obtained from a pristine PCPDTBT film is shown for comparison (green). The data confirm the selective removal of C_{71}-PCBM; the absorption features of C_{71}-PCBM are not detected in the BHJ film after soaking in alkanedithiol. We note that the red-shifted $\pi-\pi^*$ absorption band with vibronic side bands of BHJ films processed with 1,8-octanedithiol is not changed after removal of C_{71}-PCBM, indicating that the improved local structure within the PCPDTBT

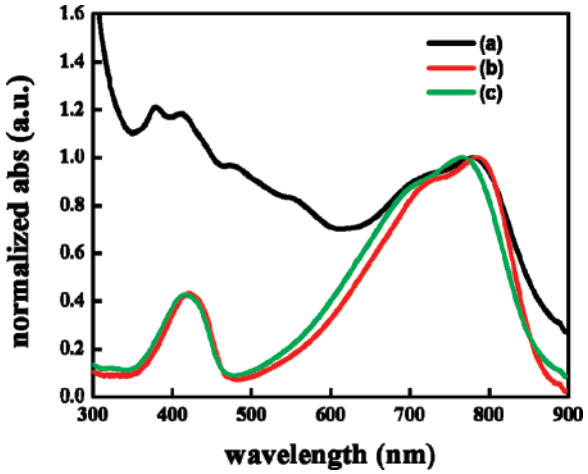

Figure 1. UV−visible absorption spectra of PCPDTBT/C_{71}-PCBM films processed with 1,8-octanedithiol: before removal of C_{71}-PCBM with alkanedithiol (black); after removal of C_{71}-PCBM with alkanedithiol (red) compared to the absorption spectrum of pristine PCPDTBT film (green).

is maintained even after removal of the PCBM. The clear observation of the morphology of the bare polymer network confirms that the selective solubility of the processing additive; the implied control of the phase separation affects both the polymer and the fullerene networks.

Thus, two criteria for processing additives for use in the fabrication of BHJ solar cells have been identified: (i) selective (differential) solubility of the fullerene component of the BHJ material and (ii) higher boiling point than the host solvent. Using these criteria, we have investigated the class of 1,8-di(R)octanes with various functional groups (R) as processing additives for BHJ solar cells and obtained the best results with 1,8-diiodooctane. The 1,8-dibromooctane functions almost as well; both 1,8-diiodooctane and 1,8-dibromooctane give better results than1,8-dithioooctane.

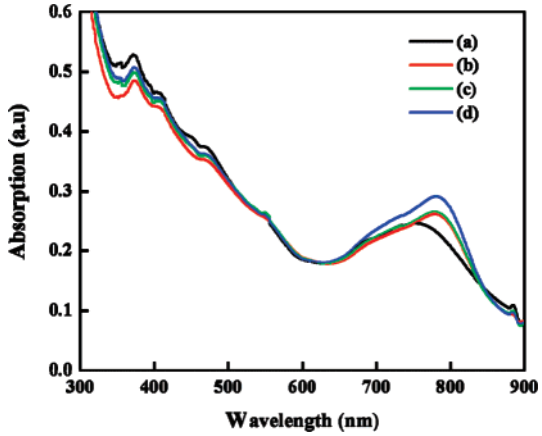

Figure 2. UV−vis spectra of (a) PCPDTBT/C_{71}-PCBM films cast from cholorobenzene and PCPDTBT/C_{71}-PCBM films cast from cholorobenzene containing 2.5% of the following: (b) 1,8-octanedithiol (red), (c) 1,8-dibromooctane (green), and (d) 1,8-diiodooctane (blue).

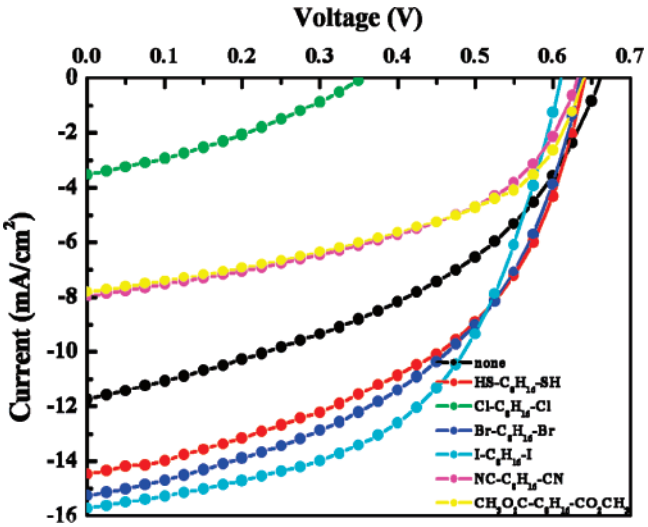

Figure 3. Current (*J*)−voltage (*V*) characteristics of PCPDTBT/C_{71}-PCBM composite films with various additives: (a) none (black), (b) 1,8-octanedithiol (red), (c) 1,8-dicholorooctane (green), (d) 1,8-dibromooctane (blue), (e) 1,8-diiodooctane (cyan), (f) 1,8-dicyanooctane (magenta), and (g) 1,8-octanediacetate (yellow).

Results and Discussion

Figure 2 shows the UV−visible absorption spectra of PCPDTBT/C_{71}-PCBM films: (a) cast from pure cholorobenzene (black curve), (b) cast from cholorobenzene containing 2.5% 1,8-octanedithiol, (c) cast from cholorobenzene containing 2.5% 1,8-diiodooctane, and (d) cast from cholorobenzene containing 2.5% 1,8-dibromooctane. Note that these films were spin-cast from solution under identical conditions with the same spin speed (2000 rpm); the absorption spectra are not normalized. As shown in Figure 2, the peak in the absorption band of PCPDTBM in the PCPDTBT/C_{71}-PCBM composite deposited from solution with the processing additives is red-shifted by 41 nm (to 800 nm) compared with that from film cast from solution without any processing additive. The $\pi-\pi^*$ absorption band intensities of the BHJ films processed using the 1,8-dibromooctane and 1,8-octanedithiol processing additives are nearly the same, but the band intensity of the BHJ film processed using 1,8-diiodooctane is higher than that of the films cast using the other additives.

Table 1. Photovoltaic Performances of the BHJ Polymer Solar Cells Composed PCPDTBT/C_{71}-PCBM Fabricated with Various Processing Additives[a]

additive	Jsc (mA/cm²)	Voc (V)	fill factor	efficiency (%)
none	11.74	0.66	0.43	3.35
HS−C_8H_{16}−SH	14.48	0.64	0.49	4.50
Cl−C_8H_{16}−Cl	3.55	0.35	0.33	0.41
Br−C_8H_{16}−Br	15.26	0.64	0.48	4.66
I−C_8H_{16}−I	15.73	0.61	0.53	5.12
NC−C_8H_{16}−CN	7.98	0.63	0.47	2.38
$CH_3O_2C-C_8H_{16}-CO_2CH_3$	7.84	0.64	0.47	2.38

[a] The optimum devices were fabricated with PCPDTBT/C71-PCBM (1:3.6) films which were spin-cast at 2.000 rpm from pristine chlorobenzene and chlorobenzene containing 2.5 vol % of additives. The performances are determined under simulated 100 mW/cm² AM 1.5G illumination. For light intensity, calibrated standard silicon solar cells with a proactive window made from KG5 filter glass traced to the National Renewable Energy Laboratory (NREL) were used. The active area of the device is 4.5 mm².

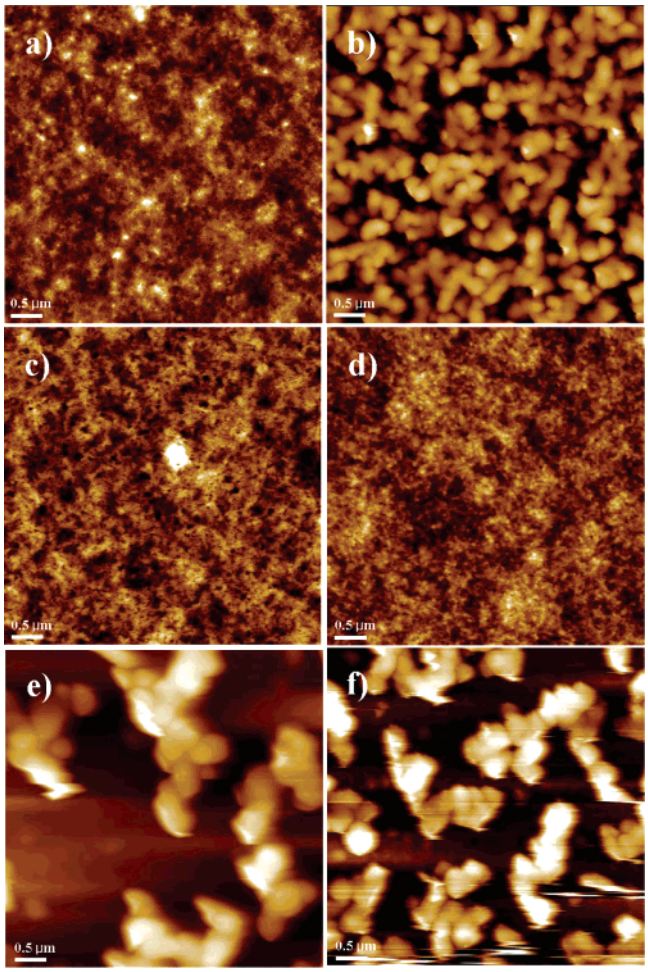

Figure 4. AFM topography of films cast from PCPCTBT/C_{71}-PCBM with additives: (a) 1,8-octanedithiol, (b) 1,8-cicholorooctane, (c) 1,8-dibromooctane, (d) 1,8-diiodooctane, (e) 1,8-dicyanooctane, and (f) 1,8-octanediacetate.

We find that photovoltaic cells based on PCPDTBT/C_{71}-PCBM processed with 1,8-diiodooctane as the processing additive exhibited the highest short circuit current (*J*sc), the highest fill factor (*FF*), and an efficiency that is approximately 10% higher than that obtained using 1,8-octanedithiol.[18] Figure 3 shows the current (*J*)−voltage (*V*) curves under AM 1.5 conditions (100 mW per cm²) of PCPDTBT/C_{71}-PCBM BHJ solar cells made using the various processing additives. The data obtained from Figure 3 are summarized in Table 1.

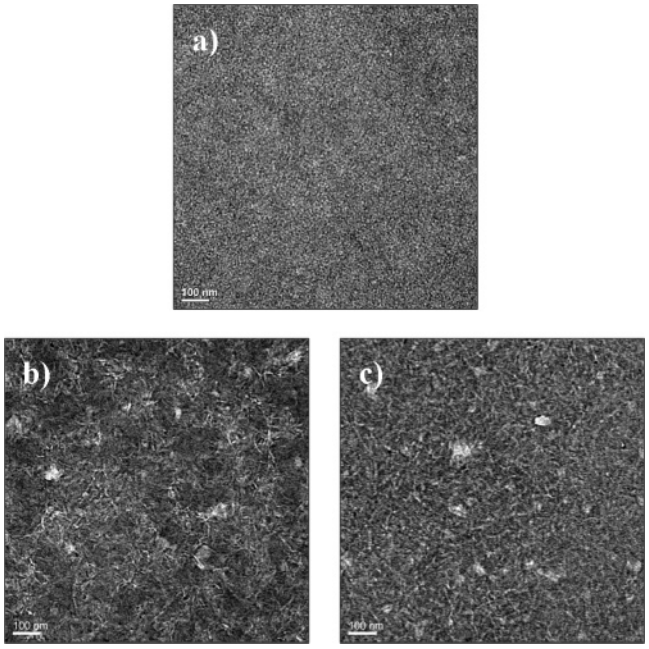

Figure 5. TEM image of films cast from PCPCTBT/C_{71}-PCBM with additives: (a) none, (b) 1,8-octanedithiol, and (c) 1,8-diiodooctane.

Performance optimization involved over 2000 devices made from over 400 independently prepared PCPDTBT/C_{71}-PCBM devices. The most efficient photovoltaic cells were fabricated using a polymer/fullerene ratio of approximately 1:3.5, a spin speed between 2000 and 2500 rpm, a polymer concentration in solution between 0.7 and 1.0 wt %, and a processing additive concentration between 2.5 and 3.0 vol % in chlorobenzene. The optimum thickness of the BHJ films obtained under these conditions was approximately 200 nm. As shown in Figure 2 and Table 1, the devices made using the 1,8-octanedithiol, 1,8-dibromooctane, and 1,8-diiodooctane exhibited enhanced *J*sc compared to films made without any processing additive, but the devices made with 1,8-dichlorooctane, 1,8-dicyanooctane, and 1,8-octanediacetate exhibited reduced *J*sc. All the processing additives (except for 1,8-dichlorooctane) caused the fill factor to increase. The most efficient devices, obtained using 1,8-diiodooctane, had an average power-conversion efficiency of 5.1% under 100 mW/cm^2, with short-circuit current $Jsc = 15.7$ mA/cm^2, fill factor $FF = 0.53$, and open-circuit voltage $Voc = 0.61$ V, i.e., an ~10% higher efficiency than that obtained with the use of 1,8-octanedithiol. Note that because of batch-to-batch variation in the quality of the PCPDTBT, the efficiency obtained using 1,8-octanedithiol was only 4.5% compared with the 5.5% reported earlier.[18] Thus, solar cells processed with 1,8-diiodooctane are expected to be capable of efficiencies above 6%.

Figure 4 shows the surface topography, measured by AFM, of films cast from PCPCTBT/C_{71}-PCBM with the various processing additives. The 1,8-octanedithiol (a), 1,8-dibromooctane (c), and 1,8-diiodooctane (d) gave phase-segregated morphologies having finer domain sizes than those obtained with 1,8-dichlorooctane (b), 1,8-dicyanooctane (e), and 1,8-octanediacetate (f). The morphology of films processed with 1,8-diiodooctane showed more elongated domains than those processed with 1,8-octanedithiol and 1,8-dibromooctane. The 1,8-di(R)octanes with SH, Br, and I, which gave finer domain sizes, exhibited more efficient device performances than those with R = Cl, CN, and CO_2CH_3. The AFM images of the BHJ films processed using 1,8-di(R)octanes with R = Cl, CN, and CO_2CH_3 showed large scale phase separation with round-shape domains and no indication of bicontinuous networks.

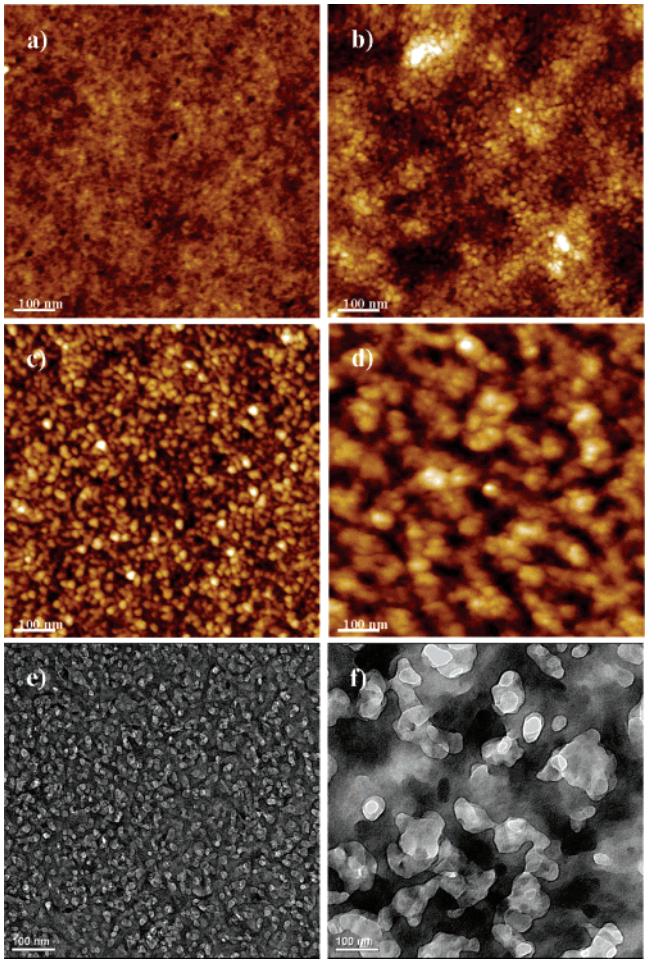

Figure 6. AFM and TEM images of BHJ films cast from PCPCTBT/C_{71}-PCBM without and with 1,8-octanedithiol and exposed PCPDTBT networks after removal of C_{71}-PCBM in BHJ film; AFM image of BHJ film (a) without and (b) with 1,8-octanedithiol; AFM image of exposed polymer networks (c) without and (d) with 1,8-octanedithiol; and TEM image of exposed polymer networks (c) without and (d) with 1,8-octanedithiol.

TEM images are shown in Figure 5. The morphology of BHJ film processed with 1,8-octanedithiol (b) and 1,8-diiodooctane (c) showed larger scale phase separation than that in the BHJ film made without using any processing additive (a). Whereas fibril-like domains are observed over the entire area of the TEM images of the BHJ films processed with 1,8-diiodooctane, these fibril-like domains are observed only in some areas of the BHJ film processed with 1,8-octanedithiol.

We have characterized the polymer networks after selectively dissolving out the fullerene from BHJ composite films using alkanedithiol. With this approach, we can directly probe the exposed polymer networks (rather than indirectly infer the regions of PCPDTBT and C_{71}-PCBM in the BHJ films using conventional AFM and TEM tools) resulting in the clear interpretation of improved charge transport and enhanced performance by processing with the additive. Figure 6 shows AFM images of BHJ films cast from PCPCTBT/C_{71}-PCBM without and with 1,8-octanedithiol and AFM and TEM images of exposed PCPDTBT networks after selective removal of C_{71}-PCBM from the BHJ film. AFM images of the BHJ films

processed with the additive exhibit larger interconnected regions of PCPDTBT and larger porous domains (the C_{71}-PCBM regions prior to selective removal) compared with images of the BHJ film cast without using the processing additive. The TEM images are consistent with the AFM results. The polymer networks and porous regions are imaged in the TEM as darker and lighter colored, respectively. The sharp, high contrast TEM images reveal that while both films contain well-connected PCPDTBT networks, the BHJ film initially cast from solution containing the processing additive showed larger areas of connectivity with larger connective cross sections. Since the short circuit current and fill factor are strongly dependent on the transport properties of the networks in the BHJ film, it is clear that, at least in part, the improved device performance results from improved hole transport as a result of the formation of the larger domains with wider connective cross sections within the PCPDTBT network.

AFM and TEM images are shown in Figures 4 and 5. After selective removal of C_{71}-PCBM from the BHJ film processed with 1,8-diiodooctane, the exposed PCPDTBT network exhibits a finer porous and fibril-like structure. After selective removal of C_{71}-PCBM from the BHJ film processed with 1,8-dichlorooctane, the exposed PCPDTBT network exhibits larger hole-like "craters" than those observed from 1,8-octanedithiol (see also Figure S3 in the Supporting Information). From these results, it becomes clear that the exposed PCPDTBT networks are closely related to the morphology of BHJ films processed with different additives. These data provide a better understanding of correlation between the polymer morphology and solar cell performance.

Conclusion

We have demonstrated the utility of a class of processing additives introduced to control the morphology of BHJ materials for use in solar cells. Two criteria for processing additives for use in the fabrication of BHJ solar cells have been identified: (i) selective (differential) solubility of the fullerene component and (ii) higher boiling point than the host solvent. The control of the BHJ morphology by selective solubility of the fullerene component in the BHJ blend was demonstrated. Using these criteria, we have investigated the class of 1,8-di(R)octanes with various functional groups (R) as processing additives for BHJ solar cells and obtained the best results with R = I or Br. Using 1,8-di-iodooctane as the processing additive, the efficiency of the BHJ solar cells was improved from 3.4% (for the reference device) to 5.1%.

Experimental Methods

The PCPDTBT and the soluble fullerene derivatives were obtained from Konarka Technologies, Inc. BHJ films were prepared under optimized conditions according to the following procedure reported previously: The indium tin oxide (ITO)-coated glass substrate was first cleaned with detergent, ultrasonicated in acetone and isopropyl alcohol, and subsequently dried overnight in an oven. Poly(3,4-ethylenedioxythiophene)/poly(styrensulfonate) PEDOT/PSS (Baytron P) was spin-cast from aqueous solution to form a film of thickness of ~40 nm. The substrate was dried for 10 min at 140 °C in air and then transferred into a glovebox to spin-cast the charge separation layer. A solution containing a mixture of PCPDTBT/C_{71}-PCBM (1:3.6) in chlorobezene with or without 2.5 vol % additives was then spin-cast on top of the PEDOT/PSS layer. A PCPDTBT network film was prepared by rinsing the PCPDTBT/C_{71}-PCBM BHJ film with alkanedithiol for 5 s. The AFM images were obtained with a Dimension 3100 atomic force microscope. TEM specimens were prepared by detaching a BHJ film from the substrate onto the surface of deionized water and picking it up with a copper grid. TEM images were obtained with a FEI T20 transmission electron microscope operated at 200 kV under proper defocus conditions.

Acknowledgment. We thank Konarka Technologies Inc. for providing the PCPDTBT and fullerene derivatives. The research was supported by Konarka Technologies and the Air Force Office of Scientific Research (Charles Lee, Program Officer). J.K.L. was partially supported by a fellowship (KRF-2006-352-C00045).

Supporting Information Available: UV−vis data, postannealing effects, AMF images, and boiling point of additives. This material is available free of charge via the Internet at http://pubs.acs.org.

JA710079W